# A Novel Architecture for Micro Fuel Cells

S. Moghaddam[*,**], E. Pengwang[*], K. Lin[**], R. Masel[**], and M. Shannon[*]

[*]Department of Mechanical Science and Engineering at University of Illinois at Urbana-Champaign,
Urbana, IL, USA, saeedmog@uiuc.edu
[**]Department of Chemical and Biomolecular Engineering at University of Illinois at Urbana-Champaign
Urbana, IL, USA

## ABSTRACT

Development of a fully integrated millimeter-scale ($3\times3\times1$ mm$^3$) fuel cell with a completely passive control mechanism is reported in this study. Fabrication of this unique power source was enabled through development of a novel self-regulating micro-hydrogen generator. The hydrogen generator stops generating hydrogen automatically when hydrogen is not consumed, enabling the micro fuel cell to operate passively, similar to a battery. The implemented passive control mechanism occupies only 0.5% of the total device volume. The first generation of this device delivered an energy density of 254 W-hr/L. Subsequent generations of this device can potentially reach 1000 W-hr/L.

***Keywords***: micro power generation, micro fuel cell, hydrogen generation, proton exchange membrane, microvalve

## 1 INTRODUCTION

The ever-increasing power demands and miniaturization of portable electronics, micro-sensors and actuators, and emerging technologies such as cognitive arthropods have created a significant interest in development of micro fuel cells. In terms of energy density, metal hydrides (e.g. $NaBH_4$), methanol, and most hydrocarbon fuels have an energy density up to an order of magnitude higher than the competitive battery technologies. Micro fuel cells, however, can potentially outperform the batteries only if their fuel to device volume ratio can be maximized and the power consumption of their auxiliary systems to regulate fuel delivery and power control is significantly reduced. While fabrication of small-scale membrane electrode assembly (MEA) is widely reported in literature [1-3], shrinking the size of the auxiliary systems (pump, valves, sensors, distribution components, and power and control electronics for these components) has remained a challenge. While this might be somewhat feasible in centimeter-scale fuel cells, fitting all the auxiliary components within a few cubic millimeters volume is quite a challenge.

Despite the advancements in fuel cell components and fabrication processing, there has been very little progress made on micro fuel cell system integration. Integrated micro-fuel cell architectures suggested in literature (e.g. in [4-7]) are scaled-downed versions of large-scale systems with numerous auxiliary components. These components can be much larger than the membrane electrode assembly (MEA), greatly reducing the overall device energy density. In addition, they consume power, which reduces available output power from the micro fuel cell for a further reduction of the device energy density. Additionally, auxiliary components normally require numerous microfabrication steps and have integration difficulties that can result in higher production costs and added complexity of micro fuel cells operation.

In this study, we report development of a fully integrated millimeter-scale fuel cell with on-board fuel and control system. Fabrication of this power source was enabled through development of a new mechanism for controlling hydrogen generation rate inside the device. The control mechanism stops generating hydrogen automatically when $H_2$ is not consumed by the fuel cell. The volume of the control mechanism is less than 50 nL (approximately 0.5% of the device volume) and requires no energy input. This technology has enabled fabrication of the first fully integrated millimeter-scale fuel cell that operates much like a battery. This technology can also be implemented in centimeter-scale micro fuel cells to enhance their energy density and reliability and reduce their complexity and cost.

## 2 OPERATION PRINCIPLE

Figure 1 shows a 3D schematic cross section of the device that consists of four layers including; 1) water reservoir, 2) membrane, 3) hydride reactor, and 4) MEA. During the device operation, water enters the narrow space between the bottom of the reservoir and the membrane (cf. Figure 2) through a gate at the bottom of the water reservoir. Capillary forces within the membrane holes keep the water from flowing into the hydride reactor. As depicted in Figure 2, water vapor diffuses into the hydride reactor. Hydrogen is generated when water vapor reacts with the hydride. The generated hydrogen then leaves the hydride reactor through a porous wall at the bottom of the reactor and reaches the MEA. If hydrogen is not used by the MEA (i.e. open circuit mode), pressure builds up inside the hydride reactor. Since the membrane is designed to deflect at a pressure less than the capillary forces within the membrane holes, it deflects and plugs the water gate thereby stopping the outflow of water from the reservoir.

The control mechanism is essentially a passive valve that automatically closes when hydrogen is not consumed. More details about the control mechanism can be found in [8].

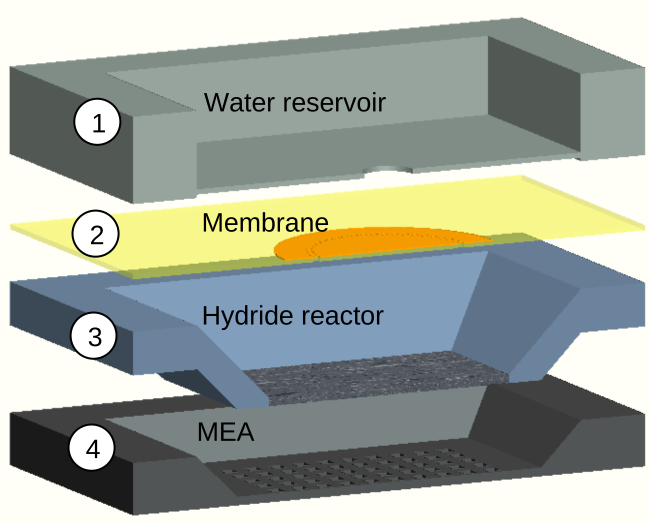

Figure 1: 3D schematic of the device assembly.

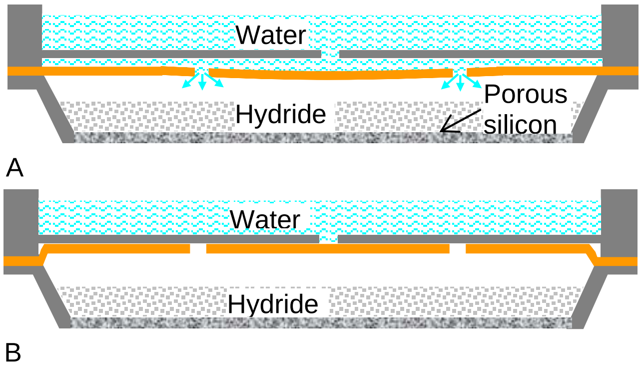

Figure 2: Schematic cross section of the self-regulating hydrogen generator and its principle of operation. A) Membrane in release mode: water exits the reservoir and diffuses into the hydride reactor through the membrane holes. B) Membrane in closed mode: small pressure buildup in the hydride reactor, when hydrogen is not used, bends the membrane and closes off the water port.

## 3 MICROFABRICATION

Details of the device microfabrication can be found in [9]. Here, a brief overview of the fabrication process is presented. The water reservoir was fabricated from <100> p-doped silicon using deep reactive ion etching (DRIE) process. The membrane separating the water chamber and the hydride reactor was made of polyimide (PI) through spinning and curing PI 5878G (from HD Microsystems) on a 100 mm diameter 500 µm thick glass wafer. The final thickness of the PI layer was 5 µm. A circular 1.3 mm diameter area at the center of the membrane was sputter coated with a 0.2 µm thick Cr/Au layer to prevent water diffusion through the membrane when it is closed. A circularly distributed array of 30 µm diameter holes was etched through the Cr/Au (wet etched) and PI (reactive ion etched) layers close to the perimeter of the Cr/Au coated area. The membrane was then transfer-bonded to the bottom of the water reservoir.

The hydride reactor was fabricated from <100> p-doped silicon using KOH etching process. The bottom wall of the hydride reactor was then anodized in 25% HF electrolyte to produce 10-20 nm in diameter pores that allow hydrogen to exit the reactor.

The hydride reactor was filled (about 60-70% of the 2.2 µL internal volume of the reactor) with $LiAlH_4$ in a glove box. The water reservoir and membrane assembly was then epoxied (using Scotch-Weld 2216 B/A Gray epoxy from 3M Co.) to the hydride reactor. Finally, the hydrogen generator was epoxied onto the MEA.

## 4 TEST RESULTS

The integrated device was tested using a Solartron SI 1287 potentiostat. The water reservoir was filled and tests were conducted. In the first test, the voltage was switched between the open circuit voltage (~0.8 V) and 0.3 V several times (i.e. square wave form), as can be seen in Figure 3. The primary goals of this experiment were the following.

1- To find out if hydrogen bubbles pass through the valve and enter the water reservoir.

2- Confirm valve closure through analysis of current transients as well as physical evidence (failure of the device due to fracture of its elements) suggesting continuous hydrogen generation and pressure build-up inside the device.

During the course of this experiment, no bubbles were observed to enter the water reservoir, indicating that the membrane deflection and capillary forces did not allow hydrogen to pass through the valve. Without the membrane, bubbles are observed to pass, even through long microchannels connecting the water reservoir to the hydride reactor. Also, the bottom wall of the water reservoir did not measurably bulge, suggesting that the hydrogen pressure did not increase measurably inside the device.

Analysis of the device current output also provided interesting insight about hydrogen generation. As can be seen in Figure 3, after 3 minutes of device not consuming any hydrogen (i.e. open circuit mode), no spike in current (beyond the steady-state value) was observed when the voltage was dropped to 0.3 V. This test suggests that hydrogen was not produced and did not accumulate inside the device when no current was drawn. Note that higher currents can be generated with increased hydrogen pressure, considering that the MEA is capable of delivering an order of magnitude higher current (700 mA/cm2 at the operating voltage of 0.3 V), than what was delivered by the integrated device. The small spike (~1 vs. 8 mA/cm2) seen in Figure 3 is mainly an artifact of the experiment. A similar negative spike can be seen when current goes to zero, which suggests the spikes are due to the measurement electronics on abrupt voltage changes. The near square-wave variation of the current generated showed that the hydrogen generation due to changes in the valve responded in less than a second.

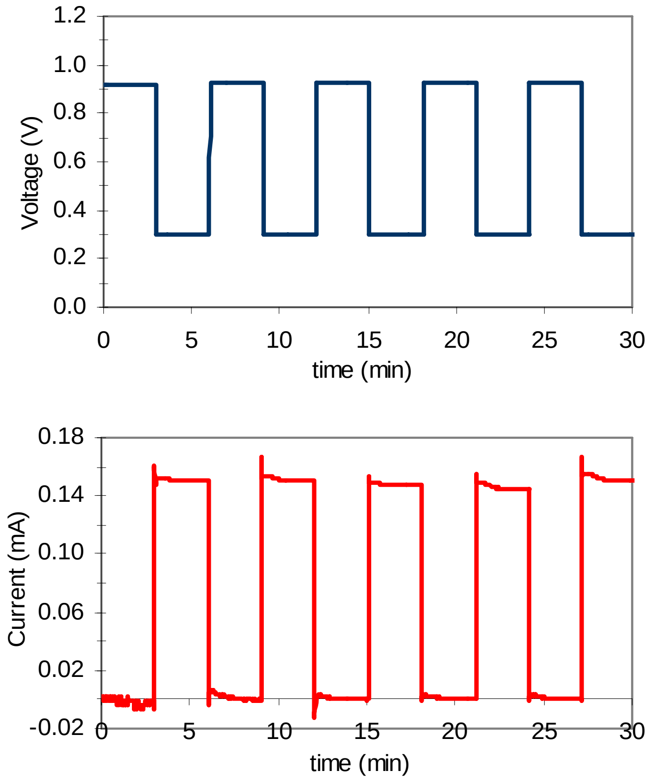

Figure 3: Device current response to voltage variations between open–circuit voltage and 0.3 V in a square wave form.

Three devices were tested to determine maximum achievable energy density. The devices were operated at 0.7 V until they ran out of fuel. Figure 4 shows the test results. The devices delivered a current of close to 0.1 mA at the beginning. Over time, however, the current decreased. We suspect this is due to reduction in hydrogen generation rate over time. One explanation could be a decrease in the water vapor rate reaching the unreacted fuel at the bottom of the hydride reactor, as thickness of the reaction products gradually increased. More research is required to clearly find the main cause of this behavior.

The energy density of the devices was between 244 to 262 W-hr/L (with an average value of 254 W-hr/L), calculated by dividing the overall generated energy (integral of the generated power reported in Figure 4) by the device volume. Considering that the hydride reactor was filled with 1.2 mg of $LiAlH_4$ (60% of the 2.22 μL reactor volume) that could generate hydrogen for 4.7 mW-hr energy (or 522.2 W-hr/L) at an operating voltage of 0.7 V, suggested that only about 49% of the fuel was utilized in the device. The rest of the fuel could have either stayed unreacted in the reactor or the generated hydrogen leaked from the device through the adhesives that may not be hydrogen impermeable. Further studies are required to quantify and minimize these losses. Achieving an energy density on the order of 400 W-hr/L is feasible with a fuel utilization efficiency of about 80%.

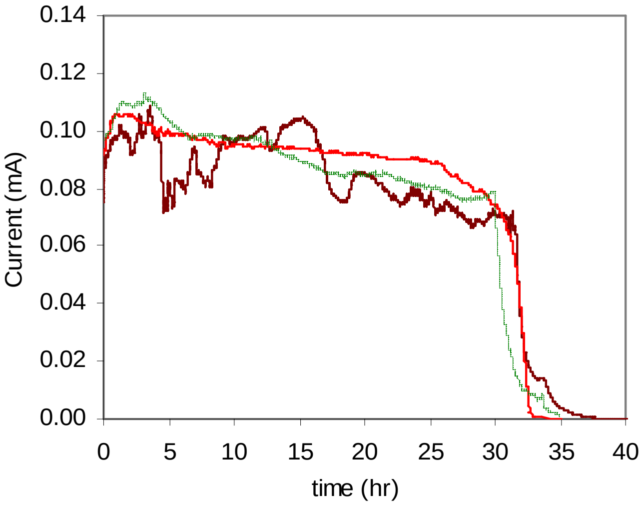

Figure 4: Current output of three devices operated at a constant voltage of 0.7 V. The overall energy density of the three devices varied from 244 to 262 W-hr/L.

Also, our calculation suggests that using the following reaction, a theoretical energy density of 756 W-hr/L at the operating voltage of 0.7 V (or 863 W-hr/L at 0.8 V) could be achieved.

$$H_2O + 0.55\ NH_4F + 0.8\ LiBH_4 \rightarrow 0.55\ LiF + 0.55\ BN + 0.25\ LiOH + 0.25\ H_3BO_3 + 3.2\ H_2$$

One challenge with this reaction is formation of compounds that are often impermeable to water vapor. We are currently conducting extensive research to resolve this issue. An energy density on the order of 700 W-hr/L can be achieved through implementation of this chemistry.

## 5 CONCLUSIONS

A fully integrated millimeter-scale fuel cell-based power source with on-board fuel and a control system was developed. Fabrication of this high energy density device in such a small volume (3×3×1 $mm^3$) was enabled through implementation of a scalable design architecture and using a novel passive control system that occupies very little volume (less than 0.5% of the device volume). Performance of the device under varying load conditions was successfully demonstrated. Simplicity of the design and microfabrication processes developed in this study has opened a new opportunity for commercialization of more cost-effective micro fuel cells.

## ACKNOWLEDGMENTS

This research is funded by the Defense Advanced Research Projects Agency (DARPA) under grant DST 2007-0299513- 000-1. Any opinions, findings and conclusions or recommendations expressed in this manuscript are those of the authors and do not necessarily reflect the views of the Defense Advanced Projects Research Agency or the US government.

# REFERENCES

[1] R. Hahn, S. Wagner, A. Schmitz, H. Reichl, "Development of a planar micro fuel cell with thin film and micro patterning technologies," J. Power Sources, 131, 73-78, 2004.

[2] T. Pichonat, B. Gauthier-Manuel, "Recent developments in MEMS-based miniature fuel cells," Microsyst. Technol., 13, 671-1678, 2007.

[3] P.J. Hesketh, J.S. Bintoro, R. Luharuka, "Microvalve for fuel cells and miniature gas chromatographic system," Sensors Update, 13, 233-302, 2004.

[4] S. Tanaka, K.-S. Change, K.-B. Min, D. Satoh, K. Yoshida, M. Esashi, "MEMS-based components of a miniature fuel cell/fuel reformer system," Chem. Eng. J., 101, 143-149, 2004.

[5] C. Xie, J. Bostaph, J. Pavio, "Development of a 2 W direct methanol fuel cell power sources," J. Power Sources, 136, 55-65, 2004.

[6] S.C. Yao, X. Yang, C.C. Hsieh, Y. Alyousef, M. Vladimer, G.K. Fedder, C.H. Amon, "Micro-Electro-mechanical Systems (MEMS)-based micro-scale direct methanol fuel cell development," Energy, 31, 636-649, 2006.

[7] W. Qian, D.P. Wilkinson, J. Shen, H. Wang, J. Zhang, "Architecture for portable direct liquid fuel cells," J. Power Sources, 154, 202-213, 2006.

[8] S. Moghaddam, E. Pengwang, R.I. Masel, M.A. Shannon, "A self-regulating hydrogen generator for micro fuel cells," J. of Power Sources, 185, 445-450, 2008.

[9] S. Moghaddam, E. Pengwang, K. Lin, R.I. Masel, M.A. Shannon, "Millimeter-scale fuel cell with on-board fuel and passive control system," J. MEMS, 17(6), 1388-1395, 2008.